Improving Wildfire Simulations by Estimation of Wildfire Wind Conditions from Fire Perimeter Measurements*

Li Tan[1], Raymond A. de Callafon[1], Jessica Block[2], Daniel Crawl[2], Ilkay Altıntaş[2]

[1] Dept. of Mechanical and Aerospace Engineering
University of California San Diego, La Jolla, CA, U.S.A.
{ltan,callafon}@eng.ucsd.edu
[2] San Diego Supercomputer Center
University of California San Diego, La Jolla, CA, U.S.A.
{jblock,lcrawl,altintas}@ucsd.edu

Abstract. This paper shows how a gradient-free optimization method is used to improve the prediction capabilities of wildfire progression by estimating the wind conditions driving a FARSITE wildfire model. To characterize the performance of the prediction of the perimeter as a function of the wind conditions, an uncertainty weighting is applied to each vertex of the measured fire perimeter and a weighted least-squares error is computed between the predicted and measured fire perimeter. In addition, interpolation of the measured fire perimeter and its uncertainty is adopted to match the number of vertices on the predicted and measured fire perimeter. The gradient-free optimization based on iterative refined gridding provides robustness to intermittent erroneous results produced by FARSITE and quickly find optimal wind conditions by paralleling the wildfire model calculations. Results on wind condition estimation are illustrated on two historical wildfire events: the 2019 Maria fire that burned south of the community of Santa Paula in the area of Somis, CA, and the 2019 Cave fire that started in the Santa Ynez Mountains of Santa Barbara County.

Keywords: Wildfire · FARSITE · Uncertainty · Interpolation · Gradient-free optimization.

1 Introduction

Fire is critical for healthy ecosystems around the world. With the increased and inevitable occurrence of wildfires, more accurate and responsive prediction of the wildfire propagation is important for resource allocation in fire fighting efforts. The fire growth modeling software FARSITE is widely used by the U.S Forest

* Work is supported by WIFIRE Commons and funded by NSF 2040676 under the Convergence Accelerator program.

ICCS Camera Ready Version 2021
To cite this paper please use the final published version:
DOI: 10.1007/978-3-030-77977-1_18

Service to simulate the propagation of wildfires [7], and is characterized by the ability to estimate the wildfire propagation under heterogeneous conditions of terrain, fuels and weather. Crucial sources of information in the modeling of fire progression are the prevailing wind conditions characterized by average wind speed and wind direction that determine the overall direction and rate of spread of the wildfire.

Considerable research has been done on studying the growth and behavior of wildfire. Rothermel introduced the mathematical model for predicting fire spread [12], and experiments have been conducted to analyse the influence of fuel and weather on the spread of fires [1]. Further steps in the study of the wildfire behavior were achieved by steering the model using real-time data [5, 10, 11]. Data assimilation by combining FARSITE and ensemble Kalman filter has been done in [6, 13–15]. Furthermore, unmanned aerial vehicles have been applied to better monitor the large-scale wildfire [9, 16]. As mentioned in [1], among the numerous factors that can affect the spread of the wildfire, wind speed and wind direction play the critical roles. Unfortunately, wind conditions are available only from sparsely placed weather stations.

Detailed studies are available on learning the (non-linear) relationship between the properties of the fuel and the wildfire progression [2–4], but often only limited information on wind speed and wind direction can be used. This means that the quality of the prediction is extremely dependent on the quality of an empirical estimate of the wind conditions obtained from geometrically spaced weather station. In reality, information of the actual wind conditions at the boundary of the wildfire is unavailable due to limited number of weather stations and the turbulent atmosphere caused by wildfire. As a result, significant and compounding errors can occur in the prediction of the wildfire propagation. A first step is to estimate the best initial wind conditions before any data assimilation procedure. In this situation, the error caused by an erroneous measurement of the wind conditions can be reduced, and the accuracy of the prediction by data assimilation techniques can be greatly improved.

In this paper a gradient-free optimization is used to provide an estimate of the initial wind conditions. The gradient-free optimization is based on iteratively refining a grid of possible wind speed and wind direction conditions and simulating wildfire progression through FARSITE. Since each grid point provides an independent wildfire simulation, the computations can be executed in parallel and also provides robustness to possible erroneous fire perimeter produced by FARSITE under certain wind conditions. For each grid, the optimal wind condition is estimated by a weighted least-squares error between a uncertainty weighted measured fire perimeter and the simulated fire perimeter. Additional refined gridding around the optimal wind conditions provides additional accuracy on the estimate. Due to the spread of the wildfire, it is highly possible that measured wildfire perimeters at different times are described by polygons with different numbers of vertexes compared to a simulated fire perimeter. Interpolation is then needed in order that different polygons have the same number of vertexes. Linear interpolation of the fire perimeters is used to guarantee the

ICCS Camera Ready Version 2021
To cite this paper please use the final published version:
DOI: 10.1007/978-3-030-77977-1_18

weighted least-squares error can always be computed. Furthermore, the weighting in the least-squares computation is adjusted to account for unevenly distributed polygons to allow an evenly distributed weighting of the complete fire perimeter.

The paper is organized as follows. Section 2 presents the polygon data model of the wildfire perimeters and the method to compare two different wildfire perimeters via a polygon interpolation and a weighted least-squares error computation. Section 3 outlines the gradient-free optimization based on iterative gridding to estimate the optimal initial wind speed and wind direction to match predicted and measured fire perimeters on the basis of the weighted least-squares error between polygons. Section 4 shows the numerical results for the estimation of wind conditions for two use cases of wildfires in California: the 2019 Maria fire that burned south of the community of Santa Paula and the 2019 Cave fire that started in the Santa Ynez Mountains of Santa Barbara County. Conclusions are summarized in Section 5.

2 Wildfire Perimeter and Error Quantification

2.1 Uncertainty Characterization

A wildfire may cover multiple disjoint burned areas. For simplicity of the analysis presented in this paper, the notion of wildfire progression is characterized by a wildfire perimeter that is considered to be a single closed polygon. The analysis presented here can be applied to each of the closed-polygons in case a wildfire does cover multiple disjoint burned areas. The single closed polygon describing the wildfire perimeter is an ordered sequence of N vertexes and N piece-wise linear line segments. The vertexes of the approximated polygon are located by the Eastern and Northern coordinate pairs $(e(k), n(k))$, $k = 1, 2, \ldots, N$.

Measurements of the wildfire perimeters can be a combined data collection effort from satellite imagery, aerial surveillance or manually mapped observations with different quality assessments [8]. Therefore, it is important to consider the two-dimensional (2D) uncertainty for each vertex of the closed polygon that describes the measured wildfire perimeter. The general description of the 2D uncertainty on a vertex $(e(k), n(k))$ is a rotated ellipse, where the semi-major axis $a(k)$, semi-minor axis $b(k)$, and the rotation angle $\alpha(k)$ collectively reflect the variance in the horizontal direction and vertical direction. Such detailed information may not be available and therefore the uncertainty on a vertex $(e(k), n(k))$ is expressed by a circle around each vertex with a radius $r(k)$, where the value of $r(k)$ is proportional to the uncertainty of the vertex on the polygon.

However, it is very likely that a measured fire perimeter comes with no uncertainty characterization. In that case, the assumption is made that the uncertainty on each vertex is proportional to the (smallest) distance to the neighboring vertex on the polygon. Formally this uncertainty is described by

$$\begin{aligned} r(k) &= \max(\min(l(k), l(k-1)), r_{min}) \\ l(k) &= \sqrt{(e(k+1) - e(k))^2 + (n(k+1) - n(k))^2} \end{aligned} \tag{1}$$

ICCS Camera Ready Version 2021
To cite this paper please use the final published version:
DOI: 10.1007/978-3-030-77977-1_18

for $k = 1, 2, \ldots, N$, where $r(k)$ is the assumed uncertainty, $l(k)$ is the distance between neighboring vertexes $(e(k+1), n(k+1))$, $(e(k), n(k))$, and r_{min} is a user-defined minimum value of uncertainty radius. The value of r_{min} is used to avoid the condition in which two adjacent vertexes are extremely close to each other, and can be determined by the accuracy of measuring method used to acquire the polygon of the fire perimeter. An illustration of the uncertainty assignment for a measured fire perimeter is given in Fig. 1.

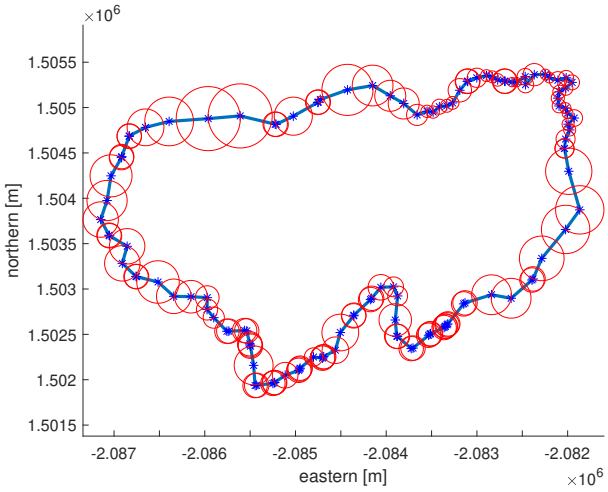

Fig. 1. Assignment of uncertainty radii $r(k)$ (circles) of a measured fire perimeter with vertexes $(e(k), n(k))$ (stars) and the resulting closed polygon (blue lines).

2.2 Perimeter Interpolation

With the spread of a wildfire, the corresponding closed polygon describing the measured fire perimeter typically becomes larger and the number N_m of vertexes of the measured closed polygon $(e_m(k), n_m(k))$, $k = 1, 2, \ldots N_m$ increases accordingly. Similarly, the number of vertexes N_s on a simulated fire perimeter $(e_s(k), n_s(k))$, $k = 1, 2, \ldots N_s$ obtained with fire modeling software such as FARSITE will also increase, but in general $N_m \neq N_s$. Next to difference in number of vertexes, the ordering of the vertexes $(e_m(k), n_m(k))$, $k = 1, 2, \ldots N_m$ of the measured fire perimeter and $(e_s(k), n_s(k))$, $k = 1, 2, \ldots N_s$ are not the same and a direct comparison between a pair $(e_m(k), n_m(k))$ and $(e_s(k), n_s(k))$ is incorrect.

The solution to this problem is to first interpolate one of the fire perimeters to the same and higher number $N = \max(N_m, N_s)$ of vertexes of the other fire perimeter. Subsequently, when comparing pairs $(e_m(k), n_m(k))$ and

ICCS Camera Ready Version 2021
To cite this paper please use the final published version:
DOI: 10.1007/978-3-030-77977-1_18

$(e_s(k), n_s(k))$, the starting vertex at $k = 1$ of one of the fire perimeters will be re-ordered to obtain the smallest weighted least-squares error between the polygons. In this paper, interpolation of the fire perimeter is done with standard 2D linear interpolation, where interpolated vertexes are introduced on the straight lines connecting the original vertexes of the closed polygon, and the procedure of linear interpolation is summarized in Algorithm 1.

Algorithm 1 Linear interpolation of wildfire polygon

Input: Vertexes of the original approximated polygon
Output: Newly constructed vertexes of the interpolated polygon

1: Calculate the length of each side of the polygon.
2: Calculate the cumulative side length from the starting point.
3: Find locations with equally distributed length along the side of polygon from the starting point.
4: Construct new polygon vertexes

Similarly, uncertainties of the original vertexes can also be interpolated with respect to the cumulative side length from the starting point. Due to the fact that the interpolation is related to the distance from the starting point, it is easy to verify that interpolation from different starting points will lead to different results. This will be considered in the subsequent section when the weighted least squares are calculated.

2.3 Weighted Least Squares Error

With an interpolated (and properly ordered) closed polygons of the simulated fire perimeter $(e_s(k), n_s(k))$, and the measured fire perimeter $(e_m(k), n_m(k))$ with an uncertainty $r(k)$ on each vertex $k = 1, 2, \ldots, N$, a weighted least-squares error

$$\frac{1}{N}\sum_{k=1}^{N} w(k)^2 \left[(e_s(k) - e_m(k))^2 + (n_s(k) - n_m(k))^2\right], \quad w(k) = \frac{1}{r(k)} \tag{2}$$

can be used to define the distance between the fire perimeters. The weighting $w(k) = 1/r(k)$ ensures measurements with a large uncertainty $r(k)$ are weighted less in the error characterization. However, even with uncertainty radii defined by (1) with a minimum value r_{min}, the weighted least-squares error in (2) will be skewed and emphasizes parts of the closed-loop polygon where vertexes are closely clustered and have only small distances with respect to each other, as also illustrated in Fig. 1. The reasons are clear:

- Small uncertainty radii $r(k)$ due to (1) will result in a larger weighting $w(k) = 1/r(k)$ on the regions of the polygon where vertexes are closely clustered.
- More vertexes in areas of the polygon where vertexes are clustered further accentuates the weighting on these regions of the polygon.

ICCS Camera Ready Version 2021
To cite this paper please use the final published version:
DOI: 10.1007/978-3-030-77977-1_18

To solve the problem of the skewed emphasis of the weighted least-squares error, the weighting $w(k)$ for each vertex is skew compensated by a weighting computed via

$$\tilde{w}(k) = w(k)c_w(k)u_w(k), \quad w(k) = \frac{1}{r(k)} \tag{3}$$

where $c_w(k)$ is a concentration weighting for each vertex used to account for clustering of vertexes on the closed polygon and the weighting $u_w(k)$ is the user-defined weighting for each vertex, used to actually emphasize certain vertexes on the closed polygon. The weighting $c_w(k)$ is defined as

$$c_w(k) = \frac{1}{m(k)} \tag{4}$$

where $m(k)$ is the number of successive vertexes around the k_{th} vertex with a small adjacent distance $l(k)$. A small adjacent distance $l(k)$ is defined by the relative distance condition

$$\frac{l(k)}{l_{mean}} < 0.2, \quad l_{mean} = \frac{1}{N}\sum_{k-1}^{N} l(k)$$

where $l(k)$ was defined in (1). The weighting $u_w(k)$ is defined to be 0 for the barrier points, defined as vertexes where the fire perimeter has not changed, and 1 for the other vertexes.

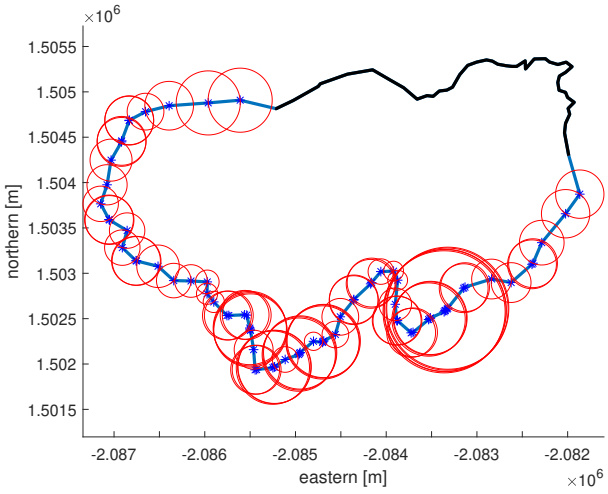

Fig. 2. Weighting radii $1/\tilde{w}(k)$ (circles) for skew-compensated least-squares compensation of a closed polygon of a measured fire perimeter consisting of vertexes $(e(k), n(k))$ (stars) and barrier vertexes (black line).

ICCS Camera Ready Version 2021
To cite this paper please use the final published version:
DOI: 10.1007/978-3-030-77977-1_18

An illustration of the skew compensation is show in Fig. 2. On account of the fact that barrier points will not move with the spread of the wildfire, a zero value weighting is assigned to each barrier point. Hence, the weighting radii of barrier points are infinitely large, and not included in Fig. 2.

Finally, to also address the re-ordering of the vertexes of the closed polygon, consider the short-hand notation based on complex numbers

$$\begin{aligned} x(k) &= e_s(k) + j \cdot n_s(k), \quad k = 1, 2, \ldots, N \\ y(k, q) &= e_m(k) + j \cdot n_m(k), \, k = q, q+1, \ldots, N, 1, \ldots, q-1 \end{aligned} \tag{5}$$

where $x(k) \in \mathbb{C}$ for $k = 1, 2, \ldots, N$ represents the 2D coordinates of vertexes of a closed polygon of a simulated fire perimeter starting at index $k = 1$ and $y(k, q) \in \mathbb{C}$ represents the 2D coordinates of vertexes of a closed polygon of a measured (and possibly interpolated) fire perimeter, but reordered to start at index q. The ability to adjust the starting point $k = q$ of the closed polygon now allows for the definition of the skew compensated weighted least-squares error

$$s = \min_q \frac{1}{N} \sum_{k=1}^{N} \tilde{w}(k)^2 |y(k, q) - x(k)| \tag{6}$$

where $\tilde{w}(k)$ is defined in (3). The starting point $k = q$ is used to remove the dependency of cyclical ordering of complex points describing the closed polygon.

3 Wind Condition Estimation with FARSITE

3.1 Forward simulations

In this study, FARSITE is used for the forward simulation of the simulated fire perimeter $x(k)$ as a function of the prevailing wind conditions u. FARSITE can be considered as a non-linear mapping $\rho(\cdot)$ for fire progression, simplified to

$$x(k) = \rho(p(k), u, \theta, \Delta_T) \tag{7}$$

where the input $p(k) \in \mathbb{C}^{N_p}$ is a closed polygon of N_p vertexes representing the initial fire perimeter. The simulated output $x(k) \in \mathbb{C}^{N_x}$, defined earlier in (5), is the closed polygon of $k = 1, 2, \ldots, N_x$ vertexes representing a simulated fire perimeter obtained after a time step of Δ_T. The additional inputs u represents the wind conditions, and θ denotes a parameter representing fuel content, fuel moisture and topography, all assumed to be constant over the time step of Δ_T.

Unknown wind conditions influence the interpolated and re-ordered vertexes of the measured fire perimeter represented by the closed polygon $y(k, q)$ defined in (5). Prevailing wind conditions in terms of wind speed and wind direction combined in a two dimensional input u will also influence the vertexes of the simulated fire perimeter represented by the closed polygon $x(k)$. Along with the definition of the weighting $\tilde{w}(k)$ in (3), it is expected that a minimization of s in (6) as a function of u will provide the best wind conditions to minimize the distance between $x(k)$ and $y(k)$.

ICCS Camera Ready Version 2021
To cite this paper please use the final published version:
DOI: 10.1007/978-3-030-77977-1_18

3.2 Wind Speed and Wind Direction Optimization

The formal problem of finding an estimate of the prevailing wind conditions on the basis of a wildfire measurement $y(k)$ can be stated as the optimization

$$\begin{aligned} \min_u s(u), \quad s(u) &= \min_q \frac{1}{N} \sum_{k=1}^{N} \tilde{w}(k)^2 |y(k,q) - x(k)| \\ x(k) &= \rho(p(k), u, \theta, \Delta_T) \end{aligned} \tag{8}$$

where $\tilde{w}(k)$ is defined in (3) and $y(k,q)$ is defined in (5). Although the $\min_q y(k,q)$ problem defined earlier in (6) is only a combinatorial problem and the optimization is a standard weighted least-squares problem, the non-linearity and non-convex mapping of $\rho(\cdot)$ requires a non-linear and iterative optimization, typically using the sensitivity or the gradient.

For FARSITE, that is responsible for the mapping in (7), the sensitivity or gradient $\frac{\partial}{\partial u}\rho(p(k), u, \theta, \Delta_T)$ is unknown. Numerical evaluation of the gradient is computationally expensive and moreover, FARSITE is known to produce occasional erroneous results at some initial wind conditions due to numerical problems in interpolation and reconstruction of the main fire perimeter (as will be shown later). These reasons motivate the use of a gradient-free optimization and the 2 dimensional size of u motivates a simple 2D gridding procedure over which $s(u)$ in (8) is evaluated. The 2D grid of u can be updated and refined iteratively to improve the accuracy of the final optimized solution for u. The pseudo-code for the iterative optimization can be summarized in Algorithm 2.

Algorithm 2 Optimizing algorithm

Input: θ, $p(k)$, $y(k)$, Δ_T, minimum wind condition perturbation λ and stopping criterion ε.

Output: Optimized $u \in \mathbb{R}^{2\times 1}$

1: Create n^2 points of a symmetric 2D grid $u_{i,j}$ over a desired range $i = 1, 2, \ldots, n$ and $j = 1, 2, \ldots, n$ around an initial estimate u_0 of the wind conditions.
2: Parallel simulation in FARSITE with $p(k)$, $u_{i,j}$, θ and Δ_T to obtain $x_{i,j}(k)$ for each grid point.
3: Compute the n^2 weighted least squares errors $s(u_{i,j})$ defined in (8) over the grid $i = 1, 2, \ldots, n$ and $j = 1, 2, \ldots, n$
4: Find the smallest value $\hat{i}, \hat{j} = \min_{i,j} s(u_{i,j})$ to select the optimized wind condition $u_{\hat{i},\hat{j}}$
5: Set $u_0 = u_{\hat{i},\hat{j}}$ and stop when $|s(u_0 + \lambda) - s(u_0)| \leq \varepsilon$ or go back to step 1 to refine grid around u_0.

The weighted least-squares error is used to determine the difference between the simulated polygon and the measured polygon of wildfire. Simulations can be performed in parallel to speed up the process of finding the optimal initial wind conditions with the above mentioned algorithm.

ICCS Camera Ready Version 2021
To cite this paper please use the final published version:
DOI: 10.1007/978-3-030-77977-1_18

4 Numerical Results

4.1 Maria Fire

The Maria Fire ignited in the evening hours of Thursday, October 31, 2019 and consumed well over 4,000 acres (16 km^2) within its first several hours of burning. The optimization of the wind conditions is performed for this fire at four different time stamps where measurements of the fire perimeter $y(k)$ were available. The objective of the optimization is to improve the fire simulations of the fire perimeters $x(k)$ with FARSITE in comparison with the observations $y(k)$ obtained at four time stamps.

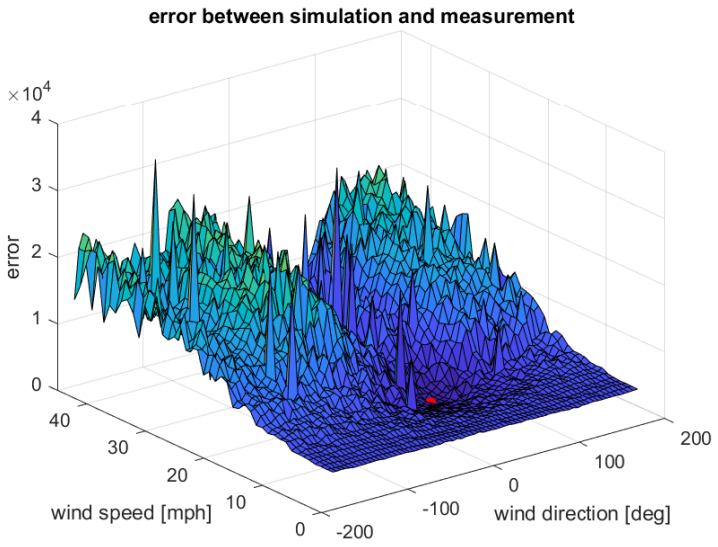

Fig. 3. Evaluation of weighted least-squares error $s(u_{i,j})$ between the simulated $x(k)$ and measured $y(k)$ fire perimeter at one particular time stamp of the Maria Fire using $n^2 = 100$ points of a symmetric 2D grid for the wind conditions $u_{i,j}$. The optimal wind condition with the lowest value of $s(u_{i,j})$ is indicated with a red dot.

First we illustrate the results of the gradient-free optimization algorithm summarized in Algorithm 2 in Fig. 3. The numerical evaluation of the weighted least-squares error $s(u_{i,j})$ over $n^2 = 100$ points of a symmetric 2D grid $u_{i,j}$ in Fig. 3 clearly shows the non-differential behavior of $s(u)$, motivating the use of a gradient-free optimization. Sporadic large values for $s(u_{i,j})$ for certain wind conditions $u_{i,j}$ are explained by erroneous results due to numerical problems in interpolation and reconstruction of the main fire perimeter by FARSITE, as illustrated in Fig. 4. The simulation results show very similar fire perimeters for two wind conditions that are very close to an erroneous result.

ICCS Camera Ready Version 2021
To cite this paper please use the final published version:
DOI: 10.1007/978-3-030-77977-1_18

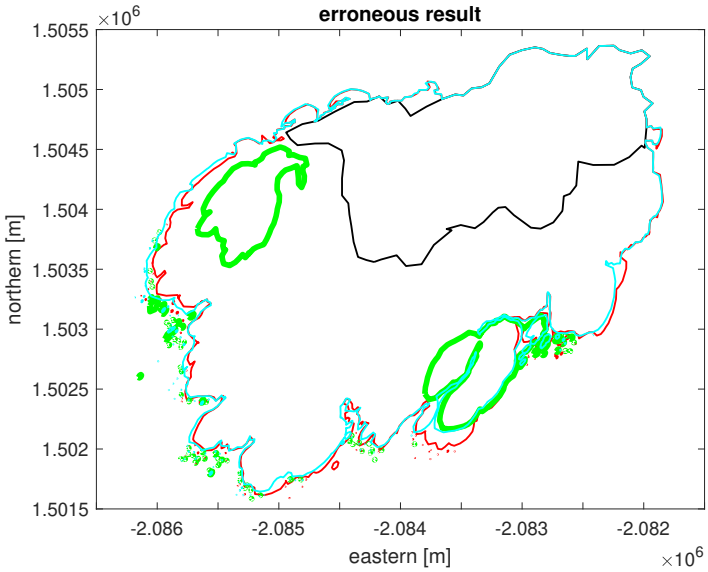

Fig. 4. Simulation of the predicted fire perimeter $x(k)$ with wind speed = 21 mph, wind direction = 34 deg (red), wind speed = 21 mph, wind direction = 35 deg (green), and wind speed = 21 mph, wind direction = 36 deg (cyan), with initial fire perimeter $p(k)$ (black).

Based on gradient-free optimization algorithm summarized in Algorithm 2, the optimization can correct wildfire simulations when the initial guesses of the prevailing wind conditions are not correct. Correction of the wildfire simulations for the four different time stamps where measurements of the Maria fire perimeter $y(k)$ were available are summarized in Fig. 5. For each time stamp, the simulated fire perimeter $x(k)$ (green lines) based on an initial estimate u_0 of the wind conditions obtained from a weather station can be improved (yellow lines) by the optimization of the wind condition via Algorithm 2. It can be observed that the optimized wind conditions provide simulations of $x(k)$ that are closer to the measurements $y(k)$ (red lines).

4.2 Cave Fire

Although the accuracy of the simulation is improved by using the optimized wind conditions, there are still some parts of the optimized simulation $x(k)$ that are somewhat far from the measurement $y(k)$. One reason may be the measurement accuracy, as the combination of aerial surveillance and manually mapped observations is likely to introduce measurement errors. It can also be observed that as the fire perimeter becomes large enough, only using a prevailing wind direction is inadequate for the accurate prediction of the wildfire propagation as wind flow is shaped by topography and atmospheric interaction.

ICCS Camera Ready Version 2021
To cite this paper please use the final published version:
DOI: 10.1007/978-3-030-77977-1_18

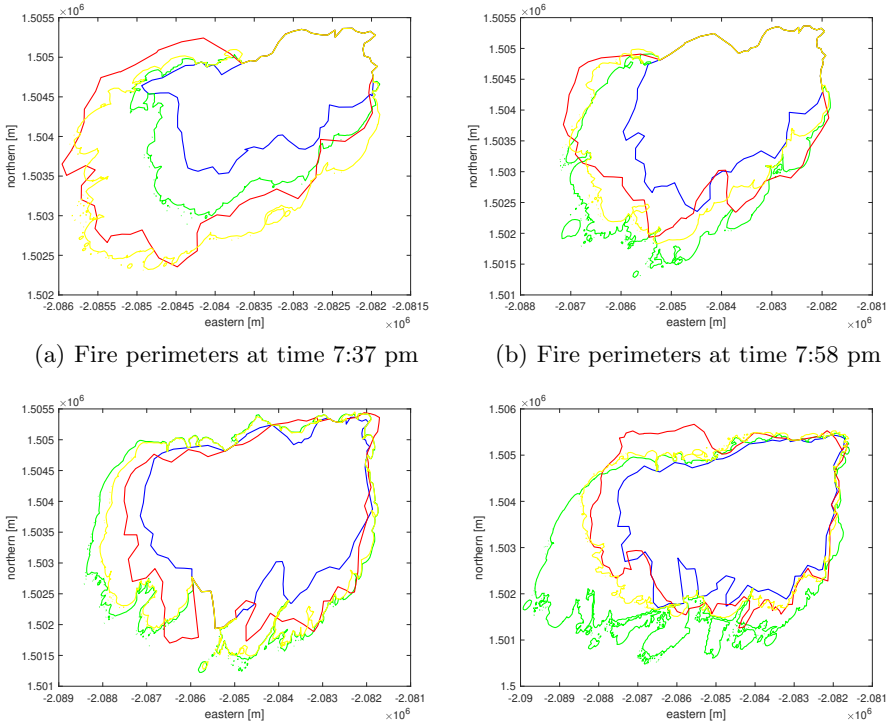

(a) Fire perimeters at time 7:37 pm

(b) Fire perimeters at time 7:58 pm

(c) Fire perimeters at time 8:31 pm

(d) Fire perimeters at time 8:56 pm

Fig. 5. Comparison of measured $y(k)$ and FARSITE simulated $x(k)$ fire perimeters for initial u_0 and optimized u wind conditions via Algorithm 2 for the Maria fire at four different time stamps. Initial ignition (blue); Simulation with initial guess u_0 (green); Simulations with optimized wind conditions u (yellow); Measurement at next time step (red).

ICCS Camera Ready Version 2021
To cite this paper please use the final published version:
DOI: 10.1007/978-3-030-77977-1_18

The measurement data available for the Cave Fire included here can better demonstrate the two issues of measurement errors and the assumption of a single prevailing wind condition. The 2019 Cave Fire started on November 25 and burned a total of 3,126 acres before being contained on December 19. As shown in Fig. 6(a), the top part of the first measurement (after the initial ignition) can be assumed to be wrongly characterized when compared to the second measurement. To be able to account for such errors on the measurement $y(k)$, the weighting radii $\tilde{w}(k)$ defined in (3) on the vertexes in the top part of the first measurement are adjusted to be zero. The effect of the weighting radii is illustrated in Fig. 6(b)) and it can be seen that the measurements in the top part of the first measurement are weighted with 0, while still allowing the remaining points $y(k)$ to be used for optimization of the prevailing wind conditions at this time stamp.

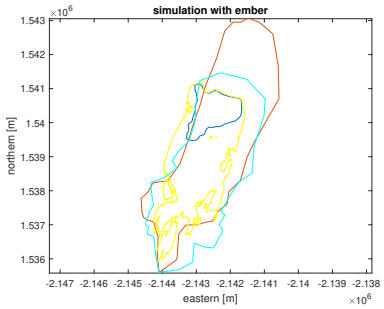

(a) Initial perimeter (blue); Measurement at the first step (red) and the second step (cyan) after the initial ignition. Simulations with optimized wind conditions (yellow);

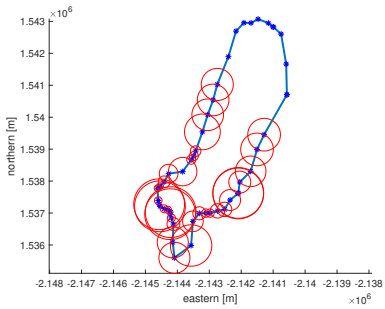

(b) Weighting radii $\tilde{w}(k)$ (red circles) on the measurement of the vertexes $y(k)$ at the first time step at 03:48 a.m (blue stars).

Fig. 6. Simulation and measurements of the Cave Fire with measurement errors in the measured fire perimeter $y(k)$ at the first time stamp after the initial fire perimeter.

When the Cave fire grows to a large dimension, as illustrated in Fig. 7, it becomes difficult to match the measured fire perimeter $y(k)$ with a simulated fire perimeter via single prevailing wind direction. The gradient-free optimization of Algorithm 2 does a better job covering the east side of the fire, but the west side of the fire cannot be covered with a single prevailing wind condition due to the topography and atmospheric wind shear effects acting on the fire. This illustrated the limitations of the proposed approach of optimizing only a prevailing wind condition.

ICCS Camera Ready Version 2021
To cite this paper please use the final published version:
DOI: 10.1007/978-3-030-77977-1_18

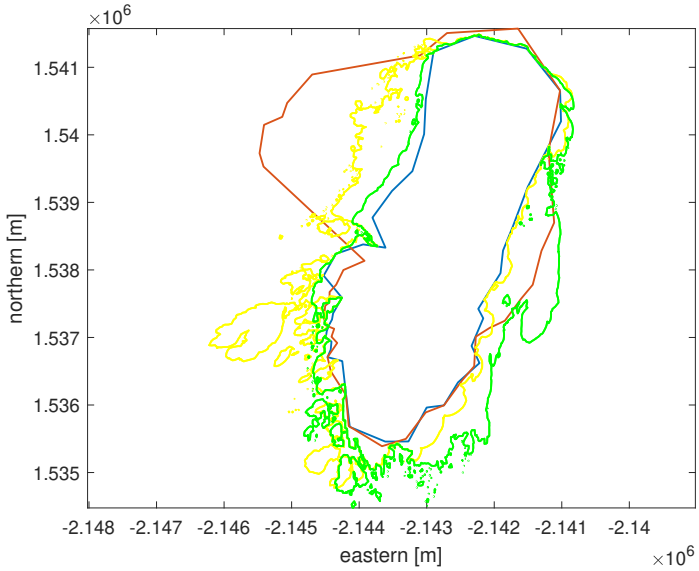

Fig. 7. Comparison of measurement $y(k)$ and FARSITE simulation when the Cave fire reaches a large dimension. Initial ignition at time 05:15 a.m (blue); Simulation with initial guess of wind conditions (green); Simulation $x(k)$ with optimized wind conditions (yellow); Measurement of fire perimeter $y(k)$ (red).

5 Conclusions

This paper shows how fire perimeter measurements can be used to improve the accuracy of a wild fire perimeter simulation, by using the measurements to estimate and correct the prevailing wind speed and wind direction for the simulation. The estimation is based on a carefully defined weighted least-squares error that measures the discrepancy between closed polygons. The weighting in the least-squares error can account for measurement accuracy, and be adjusted for a skewed weighting caused by unequally distributed vertexes on the closed polygon of the fire perimeter. Using a gradient-free optimization that exploits a grid of the two dimensional wind conditions and parallel computations with FARSITE fire modeling, optimal wind conditions are obtained by an iterative grid assignment approach. Numerical results on actual fire perimeter data obtained from two recent destructive fires in California confirm the improvement of the accuracy of a wild fire perimeter simulation. Limitations of the proposed method are due to the optimization of a single prevailing wind condition – an assumption that may not hold when a wild fire covers a large area with varying topographical features.

ICCS Camera Ready Version 2021
To cite this paper please use the final published version:
DOI: 10.1007/978-3-030-77977-1_18

References

1. Cheney, N., Gould, J., Catchpole, W.: The influence of fuel, weather and fire shape variables on fire-spread in grasslands. International Journal of Wildland Fire **3**(1), 31–44 (1993)
2. Cruz, M.G., Hurley, R.J., Bessell, R., Sullivan, A.L.: Fire behaviour in wheat crops–effect of fuel structure on rate of fire spread. International journal of wildland fire **29**(3), 258–271 (2020)
3. Cruz, M.G., Sullivan, A.L., Gould, J.S.: The effect of fuel bed height in grass fire spread: addressing the findings and recommendations of moinuddin et al. International Journal of Wildland Fire (2018)
4. Cruz, M.G., Sullivan, A.L., Gould, J.S., Hurley, R.J., Plucinski, M.P.: Got to burn to learn: the effect of fuel load on grassland fire behaviour and its management implications. International journal of wildland fire **27**(11), 727–741 (2018)
5. Douglas, C.C., Beezley, J.D., Coen, J., Li, D., Li, W., Mandel, A.K., Mandel, J., Qin, G., Vodacek, A.: Demonstrating the validity of a wildfire dddas. In: International Conference on Computational Science. pp. 522–529. Springer (2006)
6. Fang, H., Srivas, T., de Callafon, R.A., Haile, M.A.: Ensemble-based simultaneous input and state estimation for nonlinear dynamic systems with application to wildfire data assimilation. Control Engineering Practice **63**, 104–115 (2017)
7. Finney, M.A.: FARSITE, Fire Area Simulator – model development and evaluation, vol. 4. US Department of Agriculture, Forest Service, Rocky Mountain Research Station (1998)
8. Kolden, C.A., Weisberg, P.J.: Assessing accuracy of manually-mapped wildfire perimeters in topographically dissected areas. Fire Ecology **3**, 22–31 (2007)
9. Lin, Z., Liu, H.H., Wotton, M.: Kalman filter-based large-scale wildfire monitoring with a system of uavs. IEEE Transactions on Industrial Electronics **66**(1), 606–615 (2018)
10. Mandel, J., Bennethum, L.S., Chen, M., Coen, J.L., Douglas, C.C., Franca, L.P., Johns, C.J., Kim, M., Knyazev, A.V., Kremens, R., et al.: Towards a dynamic data driven application system for wildfire simulation. In: International Conference on Computational Science. pp. 632–639. Springer (2005)
11. Mandel, J., Chen, M., Franca, L.P., Johns, C., Puhalskii, A., Coen, J.L., Douglas, C.C., Kremens, R., Vodacek, A., Zhao, W.: A note on dynamic data driven wildfire modeling. In: International Conference on Computational Science. pp. 725–731. Springer (2004)
12. Rothermel, R.C.: A mathematical model for predicting fire spread in wildland fuels, vol. 115. Intermountain Forest and Range Experiment Station, Forest Service, United ... (1972)
13. Srivas, T., Artés, T., De Callafon, R.A., Altintas, I.: Wildfire spread prediction and assimilation for farsite using ensemble kalman filtering. Procedia Computer Science **80**, 897–908 (2016)
14. Srivas, T., de Callafon, R.A., Crawl, D., Altintas, I.: Data assimilation of wildfires with fuel adjustment factors in farsite using ensemble kalman filtering. Procedia Computer Science **108**, 1572–1581 (2017)
15. Subramanian, A., Tan, L., de Callafon, R.A., Crawl, D., Altintas, I.: Recursive updates of wildfire perimeters using barrier points and ensemble kalman filtering. In: International Conference on Computational Science. pp. 225–236. Springer (2020)
16. Xing, Z., Zhang, Y., Su, C.Y., Qu, Y., Yu, Z.: Kalman filter-based wind estimation for forest fire monitoring with a quadrotor UAV. In: 2019 IEEE Conference on Control Technology and Applications (CCTA). pp. 783–788. IEEE (2019)

ICCS Camera Ready Version 2021
To cite this paper please use the final published version:
DOI: 10.1007/978-3-030-77977-1_18